Wide angle lens with improved relative illumination characteristics

Zhuang, Zhenfeng, Dallaire, Xavier, Parent, Jocelyn, Roulet, Patrice, Thibault, Simon

Zhenfeng Zhuang, Xavier Dallaire, Jocelyn Parent, Patrice Roulet, Simon Thibault, "Wide angle lens with improved relative illumination characteristics," Proc. SPIE 11482, Current Developments in Lens Design and Optical Engineering XXI, 114820E (21 August 2020); doi: 10.1117/12.2570710

SPIE.

Event: SPIE Optical Engineering + Applications, 2020, Online Only

Wide angle lens with improved relative illumination characteristics

Zhenfeng Zhuang[1], Xavier Dallaire[1], Jocelyn Parent[1], Patrice Roulet[1], Simon Thibault[1,2]
[1]Immervision, 2020 University, Suite 2320, Montreal, QC, H3A 2A5 Canada
[2]Centre d'optique, photonique et laser, Département de physique, de génie physique et d'optique, Université Laval, 2375, rue de la Terrasse, Québec G1V 0A6, Canada

ABSTRACT

Consumers nowadays have a higher expectation on cameras beyond the function of taking photos or videos. In the early years, the applications of cameras with lenses were, however, very restricted. A new generation of super wide-angle lenses capture the user's surroundings in full 360°, allowing the user's friends or families to step inside our universe and experience it, live. However, for such wide angle lens coverage, the relative illumination of the lens must take the vector nature of the light into account. Consequently, the polarization of light becomes a critical parameter. Custom coatings are commonly spread on the lens surface to avoid light transmission polarization falloff. But for consumer applications, complex coating is not a practical solution because it raises cost. In this paper, we present how to take care of the polarization during the design and analysis of the lens design. Additionally, design tips are proposed to suppress the polarization impact.

Keywords: (080.3620) Lens system design; (120.4820) Optical systems; (260.5430) Polarization; (080.2740) Geometric optical design; (220.1250) Aspherics.

1. INTRODUCTION

Wide angle lenses, which produce a full field of view (FoV) larger than 180°, are widely recognized as important devices to today's lifestyles, in applications such as mobile phones, indoor environmental surveillance, car navigation and so on. The process technology has greatly improved in the past few years and consequently, the optical performance and system volume of wide-angle lenses have also improved.

There are many types of lens architecture used in wide angle lenses. The traditional fisheye lens can be traced back to the late 1924s. Although this can present a wide FoV to the user, there are some shortcomings of this structure, such as resolution loss, which is caused by the significant radial distortion when a wide or ultra-wide FoV is offered [1]. Another possibility to offer wide FoV is to use panoramic lens. However, a blind zone in the central region of the imaging plane is inevitable [2, 3]. The non-blind zone panoramic lens was created using the catadioptric configuration [4]. Owing to the complex structure and high cost, this technique is not yet widely available. A panomorph lens with wide angular FoV, high imaging resolution and refractive configuration was developed [5]. This wide angle lens can obtain a high resolution across the full FoV, but it still has some disadvantages for some of its applications. The main disadvantage is falloff of the relative illumination (RI) on the peripheral fields. Due to the large range of incoming angles of incidence on wide angle lens, a simple thin film coating couldn't work well on the meniscus shape lenses to compensate the Fresnel losses, and the cost increases are inevitable when the complex film coatings are applied.

In this paper, we present methods for enhancing relative illumination that takes the polarization effect into account in wide angle lenses without additional film coating. To explore the polarization effect, the Fresnel losses are analyzed to evaluate the factor which affect the relative illumination falloff at the image plane. Three panomorph lenses have been designed and appropriate simulations have been applied. Results demonstrate that the proposed methods are enabled to enhance RI at the peripheral fields, as well as obtain desirable optical performance.

2. POLARIZATION EFFECT ON WIDE ANGLE LENS

Figure 1 illustrates the path of light from infinity through a wide angle lens system to the image plane. Generally, these wide angle lenses include a negative refracting power front lens group and a positive refracting power rear lens group. In

Current Developments in Lens Design and Optical Engineering XXI, edited by R. Barry Johnson, Virendra N. Mahajan, Simon Thibault, Proc. of SPIE Vol. 11482, 114820E · © 2020 SPIE
CCC code: 0277-786X/20/$21 · doi: 10.1117/12.2570710

each lens element with a curved surface, incident rays are bent depending on the angle of the surface where the rays enter the lens. As a result, rays are incident into the convex meniscus lens at extremely large angles enable a large FoV.

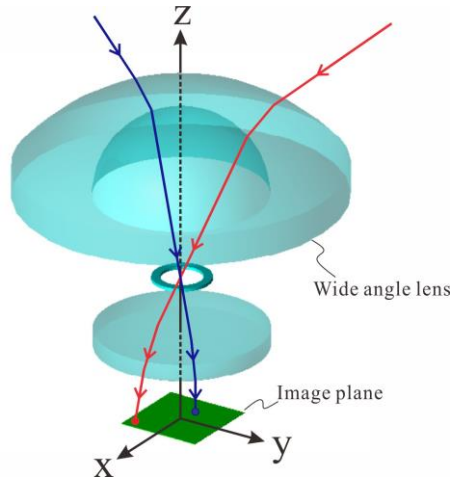

Figure 1. Schematic drawing of a wide angle lens. The incoming rays are projected onto the image plane.

Based on the electromagnetic theory, the ratio of the intensity of the reflected light to the intensity of the incident light can be determined. The polarization of the reflection and transmission of light incident on an interface of two media with different refractive index should be taken into consideration. The electric field incident into the interface can be decomposed into two orthogonal components. The vector is perpendicular to the surface of incidence is referred to as s-polarized light, and the vector is parallel to the surface of incidence is referred to as p-polarized light. The coefficients of amplitude for reflected rays (s and p) are calculated by the Fresnel equations [6], which are expressed as:

$$\begin{cases} r_s = -\dfrac{n \times \cos i - n' \cos i'}{n \times \cos i + n' \cos i'} \\ r_p = -\dfrac{n' \times \cos i - n \cos i'}{n' \times \cos i + n \cos i'} \end{cases} \tag{1}$$

where i and i' are the incident and refracted angles between two media of refractive indexes n and n'. Thus, the reflectivities of s-, p- and unpolarized light can be given by Eq. (2):

$$\begin{cases} R_s = |r_s|^2 \\ R_p = |r_p|^2 \\ R_{avg} = \dfrac{1}{2}(R_s + R_p) \end{cases} \tag{2}$$

Figure 2 shows the computed Fresnel losses for a surface of wide angle lens at the vacuum-plastic interface. At normal incidence, the s- and p-polarized waves are physically identical and have the same reflectivity of about 5.3%. As the angle of incidence increases, the reflection of s-polarized light increases gradually, while the reflection of p-polarized light decreases, until the maximum angle of incidence their values are approximately 27.7% and 1.4% of the initial intensity of the light respectively.

A graph of the reflectivities for the vacuum-plastic interface as a function of wavelength between 430 nm and 660 nm is illustrated in Fig. 3. Both s- and p-polarized lights show almost constant Fresnel losses as a function of wavelength. Nevertheless, the reflection of s-polarized light is highly sensitive to the angle of incidence. As shown in Fig. 2, at 10° incidence angle to the optical surface, the reflectivities for both s- and p-polarized light have same reflectivity, but noticeable deviation begins as the angle of incidence increases.

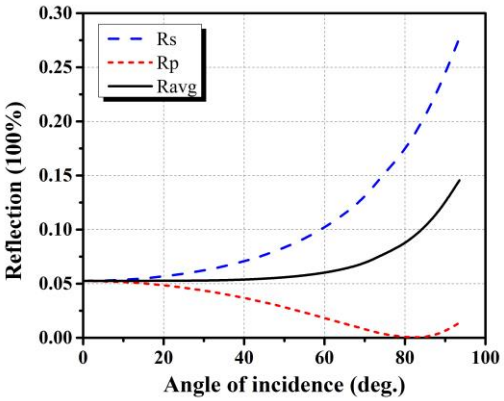

Figure 2. Fresnel reflections as a function of angle of incidence on the optical surface. Rs and Rp represent the reflectivities of the s- and p-polarized components at the interface of two media with different refractive index.

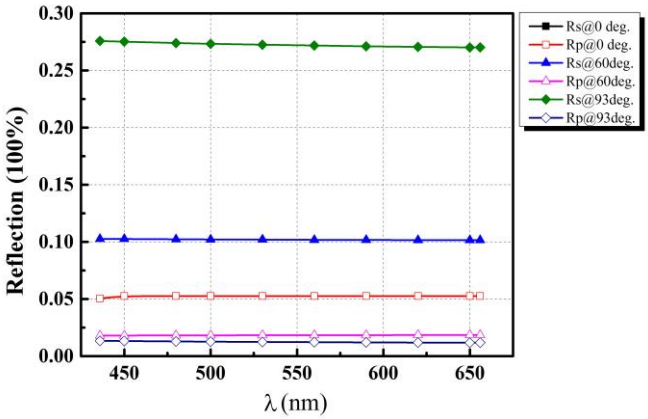

Figure 3. Fresnel reflections as a function of wavelength at optical surface.

In the case of wide angle lens, RI is one of the critical defects affecting the image performance. Since the illumination on the image plane reduces proportionally with the cosine-fourth of the angle of incidence of the chief ray to the image plane [7], the RI is prone to decrease towards the peripheral fields. Figure 4 shows the graph of RI of a wide angle lens with unpolarized and polarized effects. The RI falls off severely at the peripheral field and is about 33.6% at half FoV. However, as the RI is based on the polarization factor, the RI utilizing the polarization effect is less than 24.3% at half FoV.

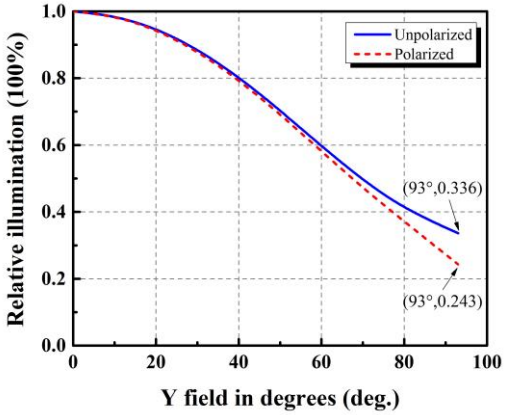

Figure 4. Relative illumination plot with unpolarized and polarized effects.

3. PRACTICAL TIPS FOR COMPENSATING FRESNEL LOSSES

Design tips are proposed in this section to compensate the RI falloff on wide angle lens. The commercial optical design software Zemax is used to verify and evaluate the performance of the wide angle lens design. Taking the polarization effect on RI into account, as an example of a complicated lens system with a large FoV and small effective focal length, three different types of panomorph lenses with 0.6 mm entrance pupil diameter, 7.5 mm total track length, 2.1 f-number, and 186° diagonal full FoV have been optimized to fulfill the present analysis purpose. The example 1 is designed using the conventional method, example 2 and 3 are designed using the incidence angle control method and the entrance pupil expanding method respectively. All of them satisfy the RMS, MTF and angular resolution design requirements. Results are analyzed and compared with each other.

3.1 Incidence angle control method

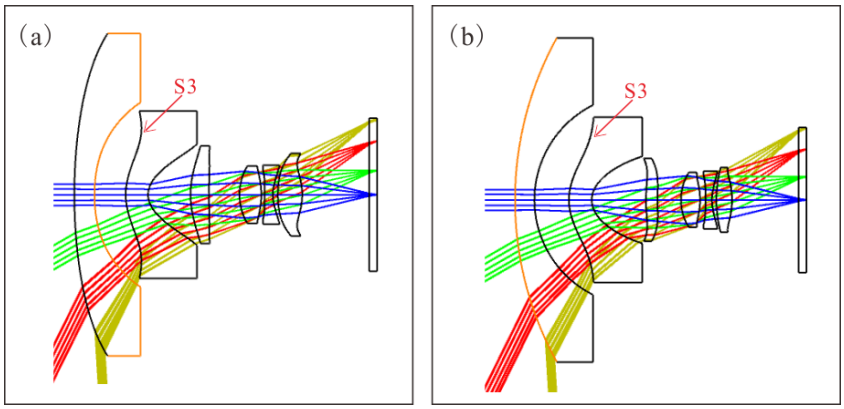

Figure 5. Ray trace through the optimized panomorph lenses. (a) Design example 1 using conventional method; (b) design example 2 using incidence angle control method.

The real ray trace through the optimized panomorph lenses are shown in Fig. 5. Figure 6 shows the Fresnel reflections as a function of angle of incidence at S3 in Fig. 5, where Fig. 6(a) represents example 1 using the conventional method in Fig. 5(a) and Fig. 6(b) represents example 2 using the incidence angle control method in Fig. 5(b). In Fig. 6(b), the reflection of s- and p-polarized lights drops considerably compared with the simulation result showed in Fig. 6(a). Figure 7 shows the corresponding RI of both design examples. It can be seen that the RI of unpolarized light remains a constant, nevertheless, the RI of polarized light increases 25.2%. As a result, using aspherical surfaces have the advantage of being very flexible for further controlling of the angle of incidence onto the refracting surfaces. Fresnel losses can be significantly reduced because of the additional degrees of freedom arising from the aspherical surfaces.

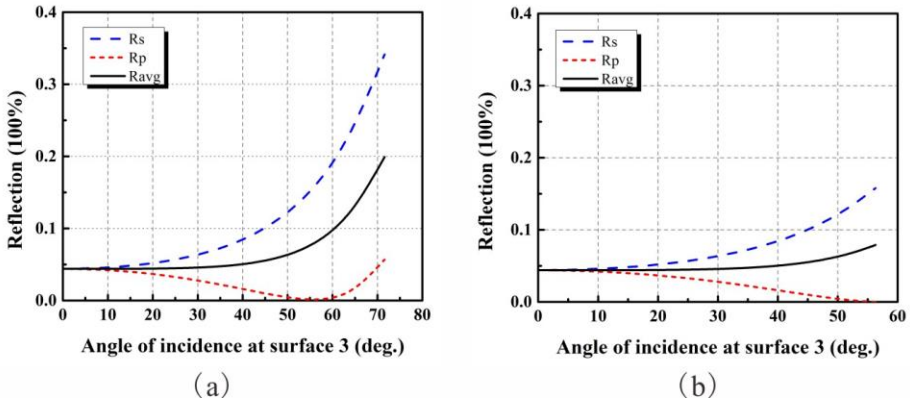

Figure 6. Fresnel reflections as a function of angle of incidence at S3. (a) conventional method; (b) incidence angle control method.

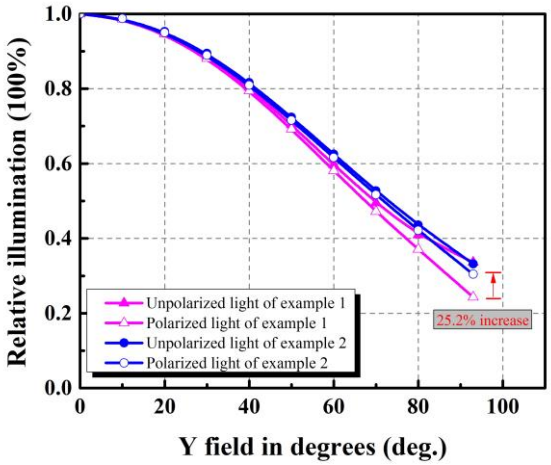

Figure 7. Relative illumination using conventional method and incidence angle control method.

3.2 Projected entrance pupil expanding method

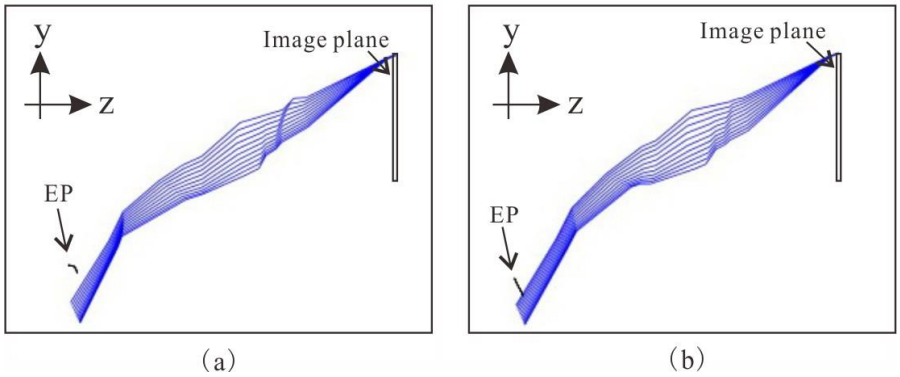

Figure. 8. Ray trace through the optimized panomorph lenses at 93° FoV. (a) Design example 1 using the conventional method; (b) design example 3 using the entrance pupil expanding method.

An alternative method to enhance the RI is to use the projected entrance pupil area. As we know, the entrance pupil position, shape and centration varies with FoVs [8,9]. According to the law of irradiance transport conservation, the irradiance distribution in image space can be expressed as:

$$E_{XP} = dS \times \cos^4 \theta \times \frac{L}{f_x f_y} \tag{3}$$

where dS is a differential area in the EP, L is the source radiance, and f_x and f_y are the focal length of the image space in the x-y and y-z planes respectively. In that case, the value of entrance pupil area is mostly in direct proportion to the RI. However, in the commercial optical design software, the off-axis entrance pupil is not provided. Here, the ray trace through the panomorph lenses and entrance pupil at 93° FoV using the conventional method and the entrance pupil expanding method are illustrated in Figs. 8(a) and 8(b) respectively. In the case of design example 3, the displacement distance for the sampled entrance pupil is close to the sampled FoV compared with the case illustrated in Fig. 8(a). Moreover, the sampled entrance pupil cannot observe obvious deformation.

The corresponding entrance pupil projection in the x-y plane is shown in Fig. 9. The blue solid line denotes the entrance pupil of example 1 in Fig. 8(a), and the red dashed line represents entrance pupil of example 3 in Fig. 8(b). It can be seen that the projected entrance pupil of example 3 is expanded in x direction, and a larger projected area can be achieved. It is noted that a large area indicates higher light intensity obtained at the image plane.

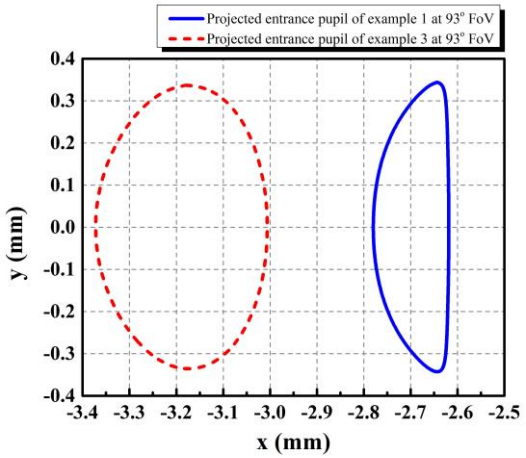

Figure 9. Projected entrance pupil in the x-y plane at 93° FoV. The solid line denotes entrance pupil of example 1, and the dash line represents entrance pupil of example 3.

To evaluate the validity of our proposed method, the RI is also used to demonstrate the level of light intensity. The pink lines represent the RI of example 1, and the blue lines represent example 3. It can be seen that not only the RI of polarized light increases but also the unpolarized light. Here, the RI of polarized light increases 46.2%.

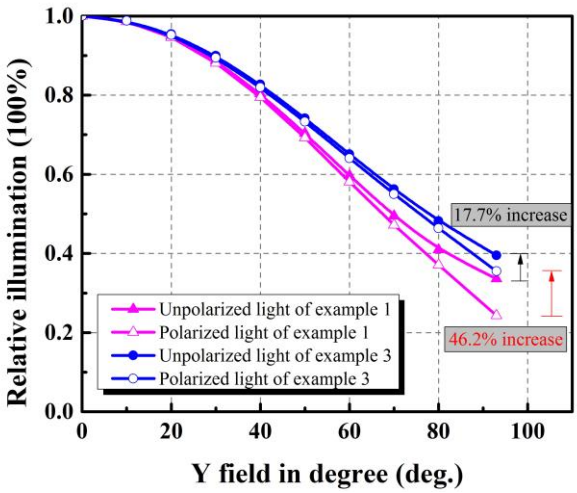

Figure 10. Relative illumination using conventional method and entrance pupil expanding method.

4. CONCLUSIONS

Design tips with the ability to alleviate the problem of low RI on the peripheral fields while maintaining the optical performance of wide angle lens are proposed. Using the proposed schemes, it is possible to directly design a wide angle lens to enhance RI with polarization effect without additional film coating.

REFERENCES

[1] E. Kose, and R. K. Perline, “Double-mirror catadioptric sensors with ultrawide field of view and no distortion,” Appl. Opt. 53(4), 528-536 (2014).
[2] Z. Huang, J. Bai, and X. Y. Hou, “Design of panoramic stereo imaging with single optical system,” Opt. Express 20(6), 6085-6096 (2012).

[3] J. H. Wang, Y. C, Liang, and M. Xu, “Design of panoramic lens based on ogive and aspheric surface,” Opt. Express 23(15), 19489-19499 (2015).
[4] D. W. Cheng, C. Gong, C. Xu, and Y. T. Wang, “Design of an ultrawide angle catadioptric lens with an annularly stitched aspherical surface,” Opt. Express 24(3), 2664-2677 (2016).
[5] S. Thibault, J. Parent, H. Zhang, and P. Roulet, “Design, fabrication and test of miniature plastic panomorph lenses with 180° field of view,” International Optical Design Conference. Optical Society of America, IM2A-3 (2014).
[6] W. Born and E. Wolf, “Basic properties of the electromagnetic field,” in Principles of Optics 7th ed. (Cambridge University Press, 1999), pp. 41–42.
[7] C. B. Martin, “Design issues of a hyper-field fisheye lens.” Proc. SPIE, 5524, 84-92 (2004).
[8] Z. F. Zhuang, S. Thibault, and J. Parent, “Analysis of three-dimensional entrance pupil model in panomorph lenses.” International Optical Design Conference. Optical Society of America (2017).
[9] Z. F. Zhuang, and S. Thibault, “Numerical investigation of three-dimensional pupil model impact on the relative illumination in panomorph lenses.” Opt. Engineering, 56(11), 115105 (2017).